

US-SFNET: A SPATIAL-FREQUENCY DOMAIN-BASED MULTI-BRANCH NETWORK FOR CERVICAL LYMPH NODE LESIONS DIAGNOSES IN ULTRASOUND IMAGES

Yubiao Yue², Jun Xue³, Haihua Liang¹, Bingchun Luo⁴, Zhenzhang Li^{1,*}

¹College of Mathematics and Systems Science,

Guangdong Polytechnic Normal University, Guangzhou, China

²School of Biomedical Engineering, Guangzhou Medical University, Guangzhou, China

³School of Computer Science and Technology, Anhui University, Anhui, China

⁴School of Computer Science and Technology, Harbin Institute of Technology, Weihai, China

ABSTRACT

Ultrasound imaging serves as a pivotal tool for diagnosing cervical lymph node lesions. However, the diagnoses of these images largely hinge on the expertise of medical practitioners, rendering the process susceptible to misdiagnoses. Although rapidly developing deep learning has substantially improved the diagnoses of diverse ultrasound images, there remains a conspicuous research gap concerning cervical lymph nodes. The objective of our work is to accurately diagnose cervical lymph node lesions by leveraging a deep learning model. To this end, we first collected 3392 images containing normal lymph nodes, benign lymph node lesions, malignant primary lymph node lesions, and malignant metastatic lymph node lesions. Given that ultrasound images are generated by the reflection and scattering of sound waves across varied bodily tissues, we proposed the Conv-FFT Block. It integrates convolutional operations with the fast Fourier transform to more astutely model the images. Building upon this foundation, we designed a novel architecture, named US-SFNet. This architecture not only discerns variances in ultrasound images from the spatial domain but also adeptly captures microstructural alterations across various lesions in the frequency domain. To ascertain the potential of US-SFNet, we benchmarked it against 12 popular architectures through five-fold cross-validation. The results show that US-SFNet is SOTA and can achieve 92.89% accuracy, 90.46% precision, 89.95% sensitivity and 97.49% specificity, respectively.

Index Terms— Ultrasound Images, Cervical Lymph Nodes, Deep Learning, Fast Fourier Transform

1. INTRODUCTION

Cervical lymph nodes play a key role in the lymphatic system, are responsible for the filtration of lymph fluid and play

a central role in immune regulation[1]. Unfortunately, it is precisely the human tissue that is prone to pathological changes. Medically, cervical lymph node lesions are divided into two categories: benign (non-neoplastic lesions) and malignant (neoplastic lesions), among which malignant lesions are further divided into primary and metastatic. Malignant lesions, in particular, are directly linked to fatal diseases such as lymphoma, head and neck cancer, and thyroid cancer, often resulting in the death of patients. Given the differences in etiology, pathological mechanism, and treatment strategy of these lesions, accurate identification and diagnosis of them has become an important task in the medical field[2]. Among various diagnostic techniques, ultrasound images is widely adopted in the evaluation of cervical lymph node lesions due to its non-invasive, real-time and low-priced advantage[3]. Unfortunately, the interpretation of ultrasound images is highly dependent on experienced radiologists, and there are still subjective differences in interpretation, which may lead to inconsistencies in diagnosis.

Recently, more and more researches have proven that compared with traditional methods, deep learning models are more efficient and accurate in ultrasound images diagnosis and even achieved accuracy exceeding radiologists. For example, Han et al. [4] used 7408 B-mode breast ultrasound images to train GoogLeNet in order to distinguish benign and malignant breast masses. They reported an accuracy of 91% for their deep learning model. Fujioka et al. [5] used 947 B-mode ultrasound images to train a model built with GoogLeNet and Inception v2, and then tested 48 images of benign masses and 72 images of malignant masses. The results showed that the accuracy of the model reaches 95.8%, which is equal to or better than that of radiologists. In addition, Yang et al. [6] collected 508 thyroid ultrasound images, and then used the pre-trained Resnet18 to analyze the benign and malignant thyroid nodules in the ultrasound images. Experimental results showed that their model was able to improve accuracy, sensitivity, F1- The scores reached 98.4%, 97.8% and 95.7% respectively. In terms of lesions

This work was supported by the NSF of Guangdong Province (No.2022A1515011044, No.2023A1515010885), and the project of promoting research capabilities for key constructed disciplines in Guangdong Province (No.2021ZDJS028). * is corresponding author.

diagnosis for cervical lymph node ultrasound images, to our knowledge, Only Xia et al. [7] collected 420 ultrasound images containing benign and malignant lesions, and then used ResNet50 and DenseNet161 to classify them. The experimental results show that DenseNet161 performed the best, and its sensitivity, specificity, accuracy and AUC reached 93%, 88%, 90% and 0.90, respectively. Simply put, the work of diagnosing lymph node lesions in cervical ultrasound images through deep learning is still in its infancy and has significant shortcomings. For example, there are the lacks of more detailed classification, sufficient validation data and exploration of model architecture.

In this work, our main contributions can be summarized as follows: (1) We collected 3392 cervical ultrasound lymph node images, covering four categories of normal lymph nodes, benign lesions, malignant primary lesions, and malignant metastatic lesions. (2) In fact, ultrasound images reflect the reflection and diffusion of sound waves by different tissues of the human body. Therefore, different tissues and lesions may exhibit characteristics in the frequency domain that are difficult to identify in the spatial domain. Taking this into account, we proposed an innovative network structure named US-SFNet. The core of the network is Conv-FFT Block, which uses identity mapping, convolution and fast Fourier transform, so that it can effectively capture the spatial and frequency domain information in ultrasound images and achieve better diagnostic results. (3) In order to evaluate the performance of the model, we adopted a five-fold cross-validation strategy. Compared with the existing 12 mainstream networks, our model achieved the most advanced performance in terms of accuracy, sensitivity, specificity and precision.

2. MATERIALS AND METHODOLOGY

2.1. Data source

The images used in this study were obtained from 480 patients who sought medical care in the radiology department of The Second Affiliated Hospital of Guangzhou Medical University from 2018 to 2021. Two radiologists used SonoScape WIS and Mindray DC-8 to collect 8 to 10 B-mode ultrasound images of neck lymph nodes from different angles for each patient, and then 2 experts eliminated the images with unqualified quality and angles to obtain 3392 images. The experts then divided these ultrasound images into four categories according to the corresponding pathological findings: normal cervical lymph nodes, benign cervical lymph nodes, malignant primary cervical lymph nodes, and malignant metastatic lymph nodes. All images are in BMP format, and the original size is $480 \times 350 \times 3$. The research protocol of this study was approved by the Review Committee of the Second Affiliated Hospital of Guangzhou Medical University (Approval No: 2022-hs-78-02). The Helsinki Declaration's

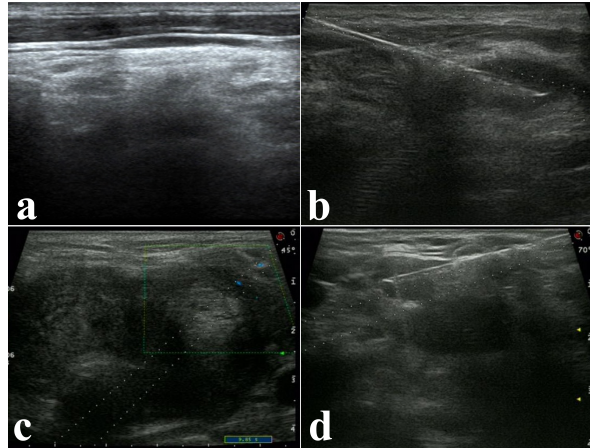


Fig. 1. The samples of different lesions. a. Normal; b. Benign; c. Primary; d. Metastatic.

tenets were scrupulously followed throughout the study to respect the rights, privacy, and anonymity of the subjects. The use of de-identified data precluded the use of informed consent.

2.2. Network Architecture

The overall framework of the model is shown in Figure 2. First, the Stem block composed of conv 3×3 , BatchNormal and GELU performs preliminary feature extraction on the input image to capture the texture and edge details in the ultrasound image and changes dimension from $3 \times 224 \times 224$ to $32 \times 112 \times 112$. Next, the backbone formed by 4 stage modules composed of Conv-FFT Block further extracts more advanced features in the image. Here, the interior of Stage1 4 is composed of [3,6,3,3] Conv-FFT Blocks respectively. In addition, between every two stages, the average pooling layer and Point-wise convolution(PW-Conv) are used to downsample the image and expand the number of channels by two times. It should be noted that two regularization modules, DropBlock[8], are followed by Stage2 and Stage3, which are used to randomly discard continuous regions in the feature map to prevent model overfitting and improve model generalization. At the end of the model, a typical classification head is used to predict the final result of the image.

Throughout the entire network architecture, Conv-FFT Block is the core component for accurate analysis of ultrasound images, and it has a unique three-branch design. The detailed structure is shown in Figure 2. From the details, the central branch is sequentially constructed by Point-wise convolution, Conv 3×3 and another Point-wise convolution, the purpose of which is to extract features from the ultrasound image in the spatial domain. In the upper branch, the feature maps first are transformed from spatial domain to frequency domain via Real Fast Fourier Transform. Next, two consecutive Conv 3×3 are used to accurately model the

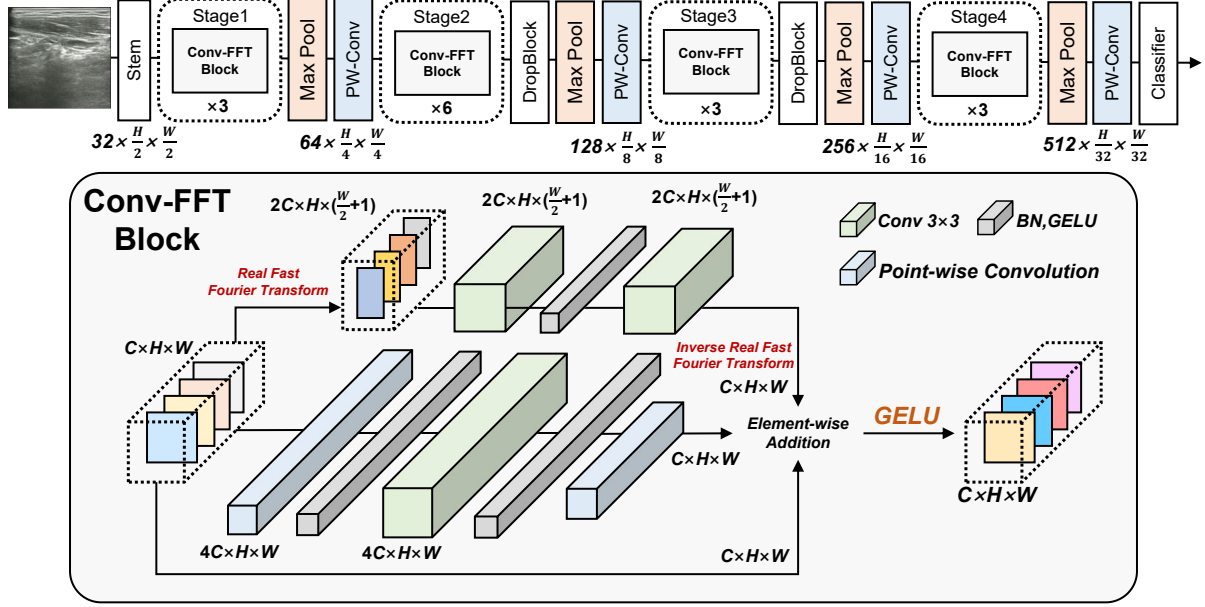


Fig. 2. The overall architecture of US-SFNet.

ultrasound image in the frequency domain and then Inverse Real Fast Fourier Transform is responsible for transforming the feature maps from frequency domain to frequency spatial domain. The lower branch adopts the strategy of identity mapping, which not only promotes the reuse efficiency of the network for features, but also effectively resists the challenge of gradient disappearance. At the end of Conv-FFT, the element-wise addition operation is used to fuse the features from the three branches, and the GELU function is used to activate the fused features to further strengthen the module's nonlinear representation of the input features.

2.3. Evaluation Metrics

Here, based on the characteristics of medical images, we have chosen to use Accuracy, Precision, Sensitivity and Specificity as evaluation metrics for the model. The high or low values of these four metrics can reflect the potential of the model in ultrasound images diagnosis. Equation (1) to Equation (4) show the calculation process of the four metrics.

$$Accuracy = \frac{TP + TN}{TP + TN + FP + FN} \quad (1)$$

$$Sensitivity = \frac{TP}{TP + FN} \quad (2)$$

$$Specificity = \frac{TN}{TN + FP} \quad (3)$$

$$Precision = \frac{TP}{TP + FP} \quad (4)$$

Here, TP, TN, FP and FN are the numbers of true positives, true negatives, false positives and false negatives.

2.4. Implementation details

In this work, we adopted a five-fold cross-validation method to thoroughly evaluate the potential of our network. The average value \pm standard deviation of the five-fold cross-validation results is used as the performance metric for the model. Before training the network, we resized all images to $224 \times 224 \times 3$. Subsequently, the images were normalized and standardized using the mean $[0.2394, 0.2421, 0.2381]$ and standard deviation $[0.2173, 0.2177, 0.2155]$ for the three channels. During the training process, we employed the Adam optimizer with a 0.001 initial learning rate, β_1 of 0.9, β_2 of 0.999, and weight decay of $1e-4$ and Cross-Entropy Loss to optimize the model parameters. We trained the model for 150 epochs, using a batch size of 64. To train the network, we utilized the PyTorch framework, and the training was conducted on a computer with Ubuntu 22.04 operating system and an NVIDIA GeForce RTX 4090 GPU.

3. RESULTS AND DISCUSSION

To demonstrate the potential and effectiveness of our work, we selected six series of well-known networks, including both Convolutional Neural Networks and Vision Transformers, as reference models. These models are DenseNet[9], ResNet[10], ConvNext[11], Swin Transformer[12] (SwinT for short), Vision Transformer[13] (ViT for short), and Swin Transformer V2 [14](SwinT V2 for short). All models were trained strictly according to the requirements specified in the implementation details, and unified metrics were used for evaluation.

Table 1. Comparison of Accuracy between US-SFNet and other networks.

| Model | Accuracy |
|----------------|-----------------------|
| US-SFNet | 92.89% (± 0.42) |
| DenseNet161 | 90.53% (± 1.11) |
| DenseNet121 | 90.59% (± 1.53) |
| ResNet101 | 86.50% (± 1.04) |
| ResNet152 | 83.90% (± 0.86) |
| ConvNext-Base | 79.54% (± 0.88) |
| ConvNext-Large | 79.83% (± 0.67) |
| SwinT-Base | 76.30% (± 0.54) |
| SwinT-Small | 76.62% (± 0.59) |
| ViT-Base | 77.27% (± 0.71) |
| ViT-Large | 75.59% (± 0.50) |
| SwinT V2-Base | 73.64% (± 1.13) |
| SwinT V2-Small | 74.20% (± 0.60) |

Table 1 shows the Accuracy, Precision, Sensitivity, Specificity and F1-S of US-SFNet and other reference models in detail. Experimental results show that our model is the best in five metrics. Meanwhile, DenseNet121, ResNet101, ConvNext-large, SwinT-small, ViT-Base and SwinT V2-small achieved the best results in their respective series. Compared with these six networks, the accuracy of US-SFNet is increased by 2.30%, 6.39%, 13.06%, 16.27%, 17.3% and 18.69%, respectively. In addition, the variance results show that US-SFNet has better stability. It is worth noting that by observing these results, an interesting phenomenon can be found: Convolutional-based architectures seem to have better advantages than Transformer-based architectures for diagnosing ultrasound image lesions. We believe this is mainly due to the fact that Transformer lacks the inherent spatial induction bias of Convolutional Neural Networks, which is precisely the key to achieving accurate classification of medical images such as cervical lymph node ultrasound images with rich details and structural information.

In order to more fully demonstrate the performance of US-SFNet, we further divide the data into Benign and non-Benign, Normal and non-Normal, Primary and non-Primary, Metastatic and non-Metastatic, and then make predictions. According to formulas 2 to 5, the Precision, Sensitivity and Specificity of US-SFNet for each type of lesion are calculated. At the same time, the best models in each series are selected for comparison. Table 2 shows in detail the diagnostic capabilities of each network for each type of disease. It is not difficult to see that US-SFNet almost shows the best Precision, Sensitivity, Specificity and F1-Score for the four lesions.

Table 2. Precision, Sensitivity, Specificity and F1-S of Different Networks for various diseases.

| Model | Type | Precision | Sensitivity | Specificity |
|----------------|------------|------------------------|------------------------|------------------------|
| US-SFNet | Benign | 85.86% (± 3.40) | 82.53% (± 2.50) | 97.02% (± 0.80) |
| | Normal | 99.51% (± 0.40) | 100.00% (± 0.00) | 99.72% (± 0.20) |
| | Primary | 84.93% (± 5.00) | 84.72% (± 5.10) | 98.83% (± 0.40) |
| | Metastatic | 91.52% (± 1.20) | 92.53% (± 0.80) | 94.40% (± 0.80) |
| DenseNet121 | Benign | 82.25% (± 7.30) | 75.87% (± 2.30) | 96.31% (± 1.90) |
| | Normal | 99.67% (± 0.60) | 99.75% (± 0.20) | 99.82% (± 0.30) |
| | Primary | 83.88% (± 6.50) | 72.87% (± 5.30) | 98.92% (± 0.50) |
| | Metastatic | 87.36% (± 1.00) | 91.99% (± 3.50) | 91.33% (± 0.70) |
| ResNet101 | Benign | 72.37% (± 4.70) | 65.90% (± 3.60) | 94.44% (± 1.50) |
| | Normal | 99.11% (± 0.90) | 99.84% (± 0.20) | 99.50% (± 0.50) |
| | Primary | 77.96% (± 7.50) | 64.45% (± 7.00) | 98.57% (± 0.60) |
| | Metastatic | 82.61% (± 0.80) | 87.51% (± 3.60) | 87.98% (± 1.00) |
| ConvNext-Large | Benign | 74.96% (± 9.80) | 30.29% (± 6.20) | 97.45% (± 1.70) |
| | Normal | 98.94% (± 0.50) | 99.67% (± 0.30) | 99.40% (± 0.30) |
| | Primary | 73.79% (± 14.40) | 26.24% (± 10.30) | 99.05% (± 0.60) |
| | Metastatic | 68.83% (± 2.00) | 93.49% (± 3.60) | 72.25% (± 3.60) |
| SwinT-Small | Benign | 68.75% (± 2.80) | 12.47% (± 1.80) | 98.78% (± 0.10) |
| | Normal | 98.78% (± 0.50) | 99.67% (± 0.30) | 99.31% (± 0.30) |
| | Primary | 25.71% (± 31.80) | 3.79% (± 4.60) | 99.84% (± 0.20) |
| | Metastatic | 63.80% (± 0.80) | 97.31% (± 0.60) | 64.02% (± 1.30) |
| ViT-Base | Benign | 61.83% (± 6.50) | 22.62% (± 3.30) | 96.92% (± 0.90) |
| | Normal | 98.07% (± 1.20) | 99.59% (± 0.20) | 98.90% (± 0.70) |
| | Primary | 54.73% (± 33.30) | 9.78% (± 7.20) | 99.40% (± 0.70) |
| | Metastatic | 66.08% (± 1.00) | 93.42% (± 0.90) | 68.74% (± 1.30) |
| SwinT V2-Small | Benign | 27.94% (± 34.30) | 2.33% (± 3.50) | 99.75% (± 0.40) |
| | Normal | 96.18% (± 0.80) | 99.26% (± 0.50) | 97.79% (± 0.50) |
| | Primary | 0.00% (± 0.00) | 0.00% (± 0.00) | 100.00% (± 0.00) |
| | Metastatic | 61.24% (± 0.50) | 96.78% (± 0.60) | 60.08% (± 1.00) |

4. COCULISON

This paper proposes a convolutional neural network based on the spatial and frequency domains for identifying lymph node lesions in cervical ultrasound images. The network surpasses state-of-the-art architectures in terms of accuracy. The next step in our research is to address the issue of dataset imbalance. Obviously, due to the existence of class imbalance, the diagnostic ability for Benign and Primary type lesions is slightly insufficient. Furthermore, we consider further testing this model in different populations according to gender and age and developing specific diagnostic systems accordingly. Additionally, we plan to explore the feasibility of conducting human-machine comparative studies, which will help evaluate the model's performance in real-world scenarios with the involvement of human expertise, thus enhancing its overall usefulness and applicability.

5. REFERENCES

- [1] Stephan Lang and Benjamin Kansy, "Cervical lymph node diseases in children," *GMS current topics in otorhinolaryngology, head and neck surgery*, vol. 13, 2014.
- [2] Anil T Ahuja, M Ying, SY Ho, G Antonio, YP Lee, AD King, and KT Wong, "Ultrasound of malignant cervical lymph nodes," *Cancer Imaging*, vol. 8, no. 1, pp. 48, 2008.
- [3] Anil T Ahuja and Michael Ying, "Sonographic evaluation of cervical lymph nodes," *AJR Am J Roentgenol*, vol. 184, no. 5, pp. 1691–9, 2005.
- [4] Seokmin Han, Ho-Kyung Kang, Ja-Yeon Jeong, Moon-Ho Park, Wonsik Kim, Won-Chul Bang, and Yeong-Kyeong Seong, "A deep learning framework for supporting the classification of breast lesions in ultrasound images," *Physics in Medicine & Biology*, vol. 62, no. 19, pp. 7714, 2017.
- [5] Tomoyuki Fujioka, Kazunori Kubota, Mio Mori, Yuka Kikuchi, Leona Katsuta, Mai Kasahara, Goshi Oda, Toshiyuki Ishiba, Tsuyoshi Nakagawa, and Ukihide Tateishi, "Distinction between benign and malignant breast masses at breast ultrasound using deep learning method with convolutional neural network," *Japanese journal of radiology*, vol. 37, pp. 466–472, 2019.
- [6] Jingya Yang, Xiaoli Shi, Bing Wang, Wenjing Qiu, Geng Tian, Xudong Wang, Peizhen Wang, and Jiasheng Yang, "Ultrasound image classification of thyroid nodules based on deep learning," *Frontiers in Oncology*, vol. 12, pp. 905955, 2022.
- [7] Limin Xia, Shanglin Lei, Huiyao Chen, and Haoyang Wang, "Ultrasound-assisted diagnosis of benign and malignant cervical lymph nodes in patients with lung cancer based on deep learning," in *International Symposium on the Frontiers of Biotechnology and Bioengineering*, 2020.
- [8] Golnaz Ghiasi, Tsung-Yi Lin, and Quoc V Le, "Drop-block: A regularization method for convolutional networks," *Advances in neural information processing systems*, vol. 31, 2018.
- [9] Gao Huang, Zhuang Liu, Laurens Van Der Maaten, and Kilian Q Weinberger, "Densely connected convolutional networks," in *Proceedings of the IEEE conference on computer vision and pattern recognition*, 2017, pp. 4700–4708.
- [10] Kaiming He, Xiangyu Zhang, Shaoqing Ren, and Jian Sun, "Deep residual learning for image recognition," in *Proceedings of the IEEE conference on computer vision and pattern recognition*, 2016, pp. 770–778.
- [11] Zhuang Liu, Hanzi Mao, Chao-Yuan Wu, Christoph Feichtenhofer, Trevor Darrell, and Saining Xie, "A convnet for the 2020s," in *Proceedings of the IEEE/CVF conference on computer vision and pattern recognition*, 2022, pp. 11976–11986.
- [12] Ze Liu, Yutong Lin, Yue Cao, Han Hu, Yixuan Wei, Zheng Zhang, Stephen Lin, and Baining Guo, "Swin transformer: Hierarchical vision transformer using shifted windows," in *Proceedings of the IEEE/CVF international conference on computer vision*, 2021, pp. 10012–10022.
- [13] Alexey Dosovitskiy, Lucas Beyer, Alexander Kolesnikov, Dirk Weissenborn, Xiaohua Zhai, Thomas Unterthiner, Mostafa Dehghani, Matthias Minderer, Georg Heigold, Sylvain Gelly, et al., "An image is worth 16x16 words: Transformers for image recognition at scale," *arXiv preprint arXiv:2010.11929*, 2020.
- [14] Ze Liu, Han Hu, Yutong Lin, Zhuliang Yao, Zhenda Xie, Yixuan Wei, Jia Ning, Yue Cao, Zheng Zhang, Li Dong, et al., "Swin transformer v2: Scaling up capacity and resolution," in *Proceedings of the IEEE/CVF conference on computer vision and pattern recognition*, 2022, pp. 12009–12019.